7-16-2018

Spectroscopy and Formation of Lanthanum-Hydrocarbon Radicals Formed by C—H and C—C Bond Activation of 1-Pentene and 2-Pentene

Wenjin Cao
University of Kentucky, wj.cao0707@uky.edu

Yuchen Zhang
University of Kentucky, yuchen.zhang@uky.edu

Silver Nyambo
University of Kentucky, Silver.Nyambo@uky.edu

Dong-Sheng Yang
University of Kentucky, Dong-Sheng.Yang@uky.edu

Right click to open a feedback form in a new tab to let us know how this document benefits you.

Follow this and additional works at: https://uknowledge.uky.edu/chemistry_facpub

Part of the Chemistry Commons, and the Physics Commons

Repository Citation

Cao, Wenjin; Zhang, Yuchen; Nyambo, Silver; and Yang, Dong-Sheng, "Spectroscopy and Formation of Lanthanum-Hydrocarbon Radicals Formed by C—H and C—C Bond Activation of 1-Pentene and 2-Pentene" (2018). *Chemistry Faculty Publications*. 131.
https://uknowledge.uky.edu/chemistry_facpub/131

Spectroscopy and Formation of Lanthanum-Hydrocarbon Radicals Formed by C—H and C—C Bond Activation of 1-Pentene and 2-Pentene

Spectroscopy and formation of lanthanum-hydrocarbon radicals formed by C—H and C—C bond activation of 1-pentene and 2-pentene

Wenjin Cao (iD), Yuchen Zhang, Silver Nyambo, and Dong-Sheng Yang (iD)

View Online   Export Citation   CrossMark

ARTICLES YOU MAY BE INTERESTED IN

Spectroscopy and formation of lanthanum-hydrocarbon radicals formed by C—H and C—C bond activation of 1-pentene and 2-pentene

Wenjin Cao, Yuchen Zhang, Silver Nyambo, and Dong-Sheng Yang[a)]
Department of Chemistry, University of Kentucky, Lexington, Kentucky 40506-0055, USA

La atom reactions with 1-pentene and 2-pentene are carried out in a laser-vaporization molecular beam source. The two reactions yield the same metal-hydrocarbon products from the dehydrogenation and carbon–carbon bond cleavage of the pentene molecules. The dehydrogenated species $La(C_5H_8)$ is the major product, whereas the carbon–carbon bond cleaved species $La(C_2H_2)$ and $La(C_3H_4)$ are the minor ones. $La(C_{10}H_{18})$ is also observed and is presumably formed by $La(C_5H_8)$ addition to a second pentene molecule. $La(C_5H_8)$ and $La(C_2H_2)$ are characterized with mass-analyzed threshold ionization (MATI) spectroscopy and quantum chemical computations. The MATI spectra of each species from the two reactions exhibit the same transitions. Adiabatic ionization energies and metal-ligand stretching frequencies are determined for the two species, and additional methyl bending and torsional frequencies are measured for the larger one. Five possible isomers are considered for $La(C_5H_8)$, and a C_1 metallacyclopentene (Iso A) is identified as the most possible isomer. $La(C_2H_2)$ is confirmed to be a C_{2v} metallacyclopropene. The ground electronic state of each species is a doublet with a La $6s^1$-based electron configuration, and ionization yields a singlet state. The formation of the lanthanacyclopentene includes La addition to the C=C double bond, La insertion into two $C(sp^3)$—H bonds, and concerted dehydrogenation. For the 2-pentene reaction, the formation of the five-membered ring may also involve 2-pentene to 1-pentene isomerization. In addition to the metal addition and insertion, the formation of the three-membered metallacycle from 1-pentene includes $C(sp^3)$—$C(sp^3)$ bond breakage and hydrogen migration from La to $C(sp^3)$, whereas its formation from 2-pentene may involve the ligand isomerization. *Published by AIP Publishing.*
https://doi.org/10.1063/1.5022771

I. INTRODUCTION

Selective metal-catalyzed activation and functionalization of C—H and C—C bonds in organic molecules are a grand challenge in chemistry. The goal of designing selective and effective metal agents for such reactions has stimulated extensive research activities in solution[1–9] and gas[10–23] phase chemistry. Gas-phase studies of metal-mediated hydrocarbon activation provide an efficient means to investigate fundamental reactivity patterns, reaction paths, and structure-reactivity relationships without interferences from solvents and counterions. Such studies are also pertinent to recent studies on single-metal-atom catalysis, which maximizes the atom efficiency of expensive metals and provides an alternative strategy to tune the activity and selectivity of a catalytic reaction.[24–36] Previous experimental studies in the gas phase were largely focused on the measurements of reaction kinetics and thermodynamics obtained with mass spectrometry-based techniques,[10–23] which are essential for understanding how metal centers activate thermodynamically stable C—H and C—C bonds. The other critical piece of information is the geometries and electronic states of reaction intermediates and products.

However, spectroscopic measurements of metal-hydrocarbon species formed through bond cleavage and coupling meet substantial challenges because the reactive species are often produced with a low number density and in electronically open shells. Although quantum chemical calculations can be used to predict the structures and electronic states for such species, a reliable prediction of low-energy electronic states and molecular structures of transition-metal or f-block organometallic species is complicated by multiple low-energy structural isomers of each species and many low-energy states or spin-orbit levels of each isomer. Therefore, a reliable identification of structural isomers and electronic states generally requires confirmation by spectroscopic measurements. Metal ion-hydrocarbon species were largely investigated with infrared or ultraviolet-visible photodissociation or photoelectron spectroscopy,[37–57] whereas metal atom-hydrocarbon radicals were mainly studied through resonant two-photon ionization and dispersed fluorescence[58–61] and Fourier transform microwave spectroscopy.[62] We have recently reported the mass-analyzed threshold ionization (MATI) spectroscopy and formation of the metal-hydrocarbon radicals produced by the lanthanide-mediated C—C and C—H bond activation of several small alkenes and alkynes.[63–71] Our studies have demonstrated that the combination of the MATI spectroscopic measurements with theoretical computations is a

---

a)Author to whom correspondence should be addressed: dyang0@uky.edu

powerful approach to investigate transient metal-hydrocarbon species.

In our previous MATI spectroscopic measurements of La reactions with ethylene,[65] propene,[67,68] and butenes,[70] we investigated the structures and formation of La-hydrocarbon radicals formed by dehydrogenation, metal insertion, and C—C bond cleavage and coupling reactions. For the La + ethylene reaction, we observed lanthanacyclopropene [La(CHCH)] from dehydrogenation and lanthanacyclopentene [La(CH$_2$CHCHCH$_2$)] from C—C bond coupling. For the propene reaction, we identified two isomers of La(C$_3$H$_4$) as methyl-lanthanacyclopropene [La(CHCCH$_3$)] and lanthanacyclobutene [La(CHCHCH$_2$)] from dehydrogenation, La(C$_3$H$_6$) as H—La(η^3-allyl) from La insertion, La(CH$_2$) as a Schrock-type metal carbene from C—C bond cleavage, and two isomers of La(C$_4$H$_6$) as lanthanacyclopentene [La(CH$_2$CHCHCH$_2$)] and trimethylenemethanelanthanum [La(C(CH$_2$)$_3$)] from C—C bond coupling. For the butene reactions, we identified the two isomers of La(C$_4$H$_6$) from the hydrogenation of 1-butene, which are the same as those from the C—C coupling of propene, but only a single isomer from the dehydrogenation of either 2-butene or isobutene. In this article, we report the MATI spectroscopy and formation of La–hydrocarbon species formed by the dehydrogenation and C—C bond cleavage of 1-pentene and 2-pentene. Pentene reactions with transition metal ions have been extensively investigated with various mass-spectrometry based measurements.[10,72–79] The general observations from these reactions are the preference of dehydrogenation, often multiple, by early transition or lanthanide ions (e.g., Sc$^+$, Ti$^+$, V$^+$, Nb$^+$, Mo$^+$, W$^+$, Gd$^+$, Pr$^+$) and the inclination of losses of ethylene and propene by later transition ions (e.g., Fe$^+$, Co$^+$, Ni$^+$). Despite the extensive early studies, electronic spectroscopy of metal-hydrocarbon species formed in such reactions is unknown, which could be used to probe state-specific structures and energetics of these reactive species that are critical for better understanding metal-mediated C—H and C—C bond activation. To our knowledge, these are the first vibronic spectroscopic measurements of metal radicals formed by the C—H and C—C bond activation of pentenes.

II. EXPERIMENTAL AND COMPUTATIONAL METHODS

The metal-cluster beam instrument used in this work consists of reaction and spectroscopy vacuum chambers and was described in a previous publication.[80] Metal-hydrocarbon reactions were carried out in a laser-ablation metal cluster beam source. 1-pentene (≥98.5%, Aldrich) or 2-pentene (cis and trans mixture, 99%, Aldrich) was seeded in a He (99.998%, Scott Gross) carrier gas with a pentene:He molar ratio of ~1 × 10^{-3} in a stainless steel mixing cylinder. La atoms were generated by pulsed-laser (Nd:YAG, Continuum Minilite II, 532 nm, ~2.0 mJ/pulse) ablation of a La rod (99.9%, Alfa Aesar) in the presence of the pentene/carrier gas mixture (40 psi) delivered by a home-made piezoelectric pulsed valve. The metal atoms and gas mixture entered into a collision tube (2 mm diameter and 2 cm length) and were then expanded into the reaction chamber, collimated by a cone-shaped skimmer (2 mm inner diameter), and passed through a pair of

deflection plates. Ionic species in the molecular beam that were formed by laser ablation were removed by an electric field (100 V cm^{-1}) applied on the deflection plates, and masses of neutral products were measured with photoionization TOF mass spectrometry.

Prior to the MATI measurements, photoionization efficiency spectra were recorded to locate an approximate ionization threshold to guide MATI scans. In the MATI experiment, metal-hydrocarbon radicals were excited to high-lying Rydberg states in a single-photon process and ionized by a delayed pulsed electric field. The excitation laser was the frequency doubled output of a tunable dye laser (Lumonics HD-500) pumped by the third harmonic output (355 nm) of a Nd:YAG laser (Continuum Surelite II). The laser beam was collinear and counter propagating with the molecular beam. The ionization pulsed field (320 V cm^{-1}), which was also used for accelerating ions into the field free region, was generated by two high voltage pulse generators (DEI, PVX-4140) and delayed by ~20 μs from the laser pulse by a delayed pulsed generator (SRS, DG645). A small dc field (6.0 V cm^{-1}) from another power supply (GW INSTEK, GPS-30300) was used to separate the ions produced by direct photoionization from the MATI ions generated by delayed field ionization. The MATI ion signal was obtained by scanning the tunable dye laser, detected by a dual microchannel plate detector, amplified by a preamplifier (SRS, SR445), visualized by a digital oscilloscope (Tektronix TDS 3012), and stored in a laboratory computer. Laser wavelengths were calibrated against titanium atomic transitions in the MATI spectral region, and the calibration was done after recording the MATI spectra.[81] The Stark shift on the adiabatic ionization energy (ΔAIE) induced by the dc field (E$_f$) was calculated using the relation of ΔAIE = 6.1E$_f^{1/2}$, where E$_f$ is in V cm^{-1} and ΔAIE is in cm^{-1}.[82]

The density functional theory (DFT) method with the B3LYP hybrid functional[83] was used to calculate the equilibrium geometries and vibrational frequencies of La(C$_5$H$_8$), La(C$_2$H$_2$), and the free ligands. The basis sets used in these calculations were 6-311+G(d,p)[84] for C and H and the Stuttgart/Dresden (SDD)[85] effective-core-potential basis set with 28-electron core for La. We have extensively used the DFT/B3LYP method and found that this method generally produced adequate results for spectral and structural assignments of organometallic radicals.[63–70,86] No symmetry restrictions were imposed in initial geometry optimizations, but appropriate point groups were used in subsequent optimizations to help identify electronic symmetries. The geometry of each stationary point was obtained through a relaxed potential energy surface scan along the proposed reaction coordinates. The relaxed scan involved the scanning of bond distances for bond breakage or dihedral angles for atom or group reorientation, and the structure of each point of the scan was optimized using the Berny algorithm. For each optimized stationary point, a vibrational analysis was performed to identify the nature of the stationary point (minimum or saddle point). Energy minima connected by a transition state were confirmed by intrinsic reaction coordinate calculations. All calculations were performed with the Gaussian 09 software package.[87]

To compare with the experimental MATI spectra, multi-dimensional Franck-Condon (FC) factors were calculated from the equilibrium geometries, harmonic vibrational frequencies, and normal coordinates of the neutral and ionized complexes.[88] In these calculations, the recursion relations from the study of Doktorov *et al.*[89] were employed, and the Duschinsky effect[90] was considered to account for a possible axis rotation from the neutral complex to the cation. Spectral simulations were obtained using the experimental line width and Lorentzian line shape. Transitions from excited vibrational levels of the neutral complex were considered by assuming thermal excitation at specific temperatures.

III. RESULTS AND DISCUSSION

A. TOF mass spectra and La-hydrocarbon species

Figure 1 displays the TOF mass spectra of the ablated La beam seeded in pure He (a) and La reactions with 1-pentene (b) and 2-pentene (c). The mass spectrum with He shows a strong LaO peak and a small La atomic peak. The weak atomic peak is largely due to its IE (5.5769 eV) that is higher than the single photon energy. Because of low ablation laser power, no La clusters were produced except for very small amounts of La_2, La_2C, and $La_2O_{1,2}$. La oxides could be formed by La reactions with oxygen that is present in the carrier gas as an impurity or by laser vaporization of La oxide impurity in the La rod,[63–69] whereas the La carbide could be associated with La reactions with the vapor of diffusion pump oil. The mass spectra from the two pentene reactions are essentially the same and show a predominant product $La(C_5H_8)$, a significant amount of La $(C_{10}H_{18})$, and two minor species $La(C_2H_2)$ and $La(C_3H_4)$. LaO is still present in the spectrum, but its intensity is weaker than that with He only. The reduced amount of LaO is likely due to the La reaction with pentene molecules, which reduces the number of La atoms available for the $La + O_2$ reaction to form LaO. $La(C_5H_8)$ is formed by the loss of H_2 from pentenes, and $La(C_2H_2)$ and $La(C_3H_4)$ are formed by the C—C cleavage of the pentene molecules with the loss of propane or ethane. $La(C_{10}H_{18})$ is presumably an adduct formed by the reaction of $La(C_5H_8)$ with a second pentene molecule [i.e., $La(C_5H_8)(C_5H_{10})$]. The observation of predominating H_2 loss is similar to previous studies on pentene reactions with early transition metal ions, except that the metal ion-mediated reactions yielded two or more H_2 losses.[10,75,79] In Secs. III B and III C, we will discuss the MATI spectra and formation of $La(C_5H_8)$ and $La(C_2H_2)$. We also attempted MATI measurements on $La(C_3H_4)$ and $La(C_{10}H_{18})$ but were not successful in obtaining sharp spectra. The failure of the MATI measurement on $La(C_3H_4)$ is largely due to the extremely low number density of this species, as sharp spectra were recorded for the species of the same stoichiometry formed in the La reaction with propene.[67] The reason for the lack of the MATI spectrum of $La(C_{10}H_{18})$ is less clear. But, it could be due to a large geometry change upon ionization that leads to FC transitions with a weak origin band and weak vibronic bands at low vibrational quanta, an unfavorable case for the MATI experiment. It could also be due to photon-induced dissociation of the complex.

B. MATI spectroscopy, structure, and formation of $La(C_5H_8)$

MATI spectra of $La(C_5H_8)$ formed by the La reactions with 1-pentene and 2-pentene are essentially the same as shown in Fig. 2, though the spectrum from the 1-pentene reaction [Fig. 2(a)] has a slightly better signal/noise ratio than that from the 2-pentene reaction. Both spectra exhibit a strong origin band at 38 984 (5) cm^{-1} and several weak bands. The weak transitions at the higher energy side of the origin band consist of 410 and 290 cm^{-1} progressions, each with up to two vibrational quanta, as well as 165 and 130 cm^{-1} bands, and those at the lower energy side include 402, 268, 156, and 128 cm^{-1} bands. Transitions marked with "∗" and "#" are combination bands of 410 + 130 cm^{-1} and 410 + 290 cm^{-1}, respectively.

Five low-energy isomers of $La(C_5H_8)$ (Fig. 3 and Table I) are predicted by the DFT/B3LYP calculations. Iso A and Iso B are both five-membered metallacycles with a methyl
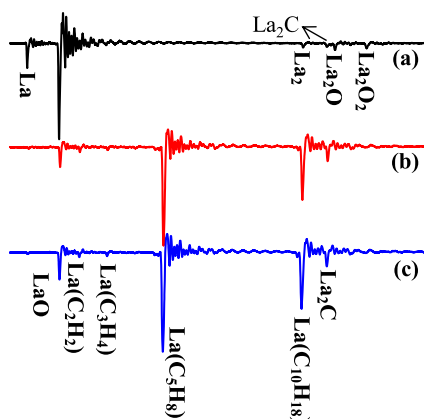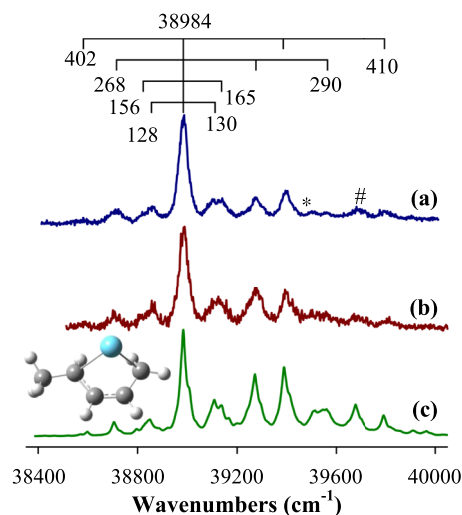

FIG. 1. TOF Mass spectra of La + He (a), La + 1-pentene/He (b), and La + 2-pentene/He (c) recorded with 239 nm photoionization. The molar ratio of pentene:He in each mixture is ~1 × 10⁻³.

FIG. 2. MATI spectra of $La(C_5H_8)$ produced from La reactions with 1-pentene [(a), blue] and 2-ptentene [(b), dark red] and the simulation of the $^1A \leftarrow {}^2A$ transition of $La(C_5H_8)$ (C_1) (Iso A) at 300 K [(c), green]. Bands marked with "∗" and "#" are combination bands.
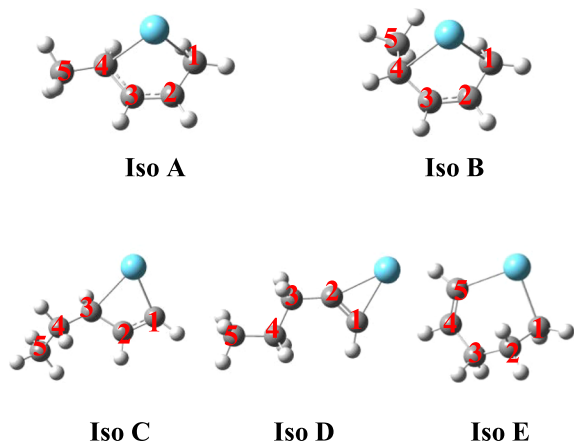
FIG. 3. Structures of five La(C_5H_8) isomers. Relative energies of these isomers are listed in Table I.

substitution of a H atom on terminal ring-C atoms. The main difference between the two conformational isomers is the orientation of the CH_3 group relative to the adjacent CH_2 group, which is staggered in Iso A but eclipsed in Iso B. Like an ethane molecule, the eclipsed form is slightly less stable than the staggered form (by ~2.0 kcal mol^{-1}) because in the eclipsed form the orbitals of the C—H bonds in the methyl group has the least amount of overlap with the C—H (or C—La or C—C) orbitals of the adjacent carbon. Iso C is a four-membered metallacycle with an ethyl substitution, whereas Iso D is a three-membered ring with a propyl substituent. Iso E is a six-membered ring with La binding to two terminal carbon atoms of pentene and is ~14.5 kcal mol^{-1} higher in energy than Iso A. The six-membered ring is more like a boat conformation with the average C—C bond distance of 1.484 Å, ~0.05 Å longer than the average bond distance (1.439 Å) in Iso A. These metallacycles may be considered hetero cycloalkenes in which the heteroatom is the La atom. As expected from the viewpoint of molecular strain energy, the five-membered rings are more stable than the four-membered one, and the four-membered

ring is more stable than the three-membered one. The hydrocarbon moiety in each of the metallacycles can be considered as a diradical, with an unpaired C $2p\pi$ electron on either of the La-bonded C atoms. Because the ground electron configuration of La atom ($5d^1 6s^2$) is not reactive toward hydrocarbon compounds, a La 6s electron is promoted to a 5d orbital to yield a reactive La $5d^2 6s^1$ configuration. The unpaired C $2p\pi$ electrons on the La-bonded C atoms are each paired with a La 5d electron to form two La—C σ bonds. Thus, the ground electronic state of each lanthanacycle is expected to be a doublet with a La 6s-based electron in the highest occupied molecular orbital. Removal of the La 6s electron by ionization yields a singlet ion.

Ionization of Iso A produces an singlet ion with its structure similar to that of the neutral species (Table S1 of the supplementary material) and is responsible for the observed MATI spectra of La(C_5H_8) formed by both 1-pentene and 2-pentene reactions. This assignment is supported by the good agreement between the simulation of the $^1A \leftarrow {}^2A$ transition of Iso A [Fig. 2(c)] and experimental spectra [Figs. 2(a) and 2b]. The origin band in the simulation is aligned with those in the experimental spectra, but the computed vibrational frequencies are unscaled in order to directly compare with the experimental observations. Based on the spectral simulation, the 410/402 and 290/268 cm^{-1} bands are assigned to the symmetric (ν_{30}^+/ν_{30}) and asymmetric (ν_{32}^+/ν_{32}) metal-ligand stretching excitations, and the 165/156 and 130/128 cm^{-1} bands are attributed to the CH_3 torsional (ν_{35}^+/ν_{35}) and bending (ν_{36}^+/ν_{36}) motions in the $^1A/^2A$ states, respectively (Table II). We have also considered possible contributions from Iso B, C, D, and E to the observed spectra but excluded them by the following considerations: The MATI spectra would have shown a second band system if they had contributions from any of these four isomers. However, the spectra show no sign of an additional band system. Simulations of Iso B, C, D, and E are not consistent with the observed spectra, as shown by Fig. S1 of the supplementary material. These isomers are all predicted to be at higher energies, which could either be quenched by supersonic expansions if they were formed or would have different ionization energies.

TABLE I. Molecular point groups, electronic states, and relative energies (cm^{-1}) of La(C_2H_2) and five isomers of La(C_5H_8) from DFT/B3LYP calculations. The energies of Iso B, C, D, and E are relative to that of Iso A. All energies include vibrational zero point energy corrections.

Complex	Point group	State	Energy
La(C_2H_2)	C_{2v}	$^2A_1$	0
	C_{2v}	$^1A_1$	42 107
La(C_5H_8), iso A	C_1	^2A	0
	C_1	^1A	39 675
La(C_5H_8), iso B	C_1	^2A	694
	C_1	^1A	39 099
La(C_5H_8), iso C	C_1	^2A	1 939
	C_1	^1A	41 513
La(C_5H_8), iso D	C_s	$^2A'$	3 172
	C_s	$^1A'$	42 836
La(C_5H_8), iso E	C_1	^2A	5 068
	C_1	^2A	44 450

TABLE II. Adiabatic ionization energies (AIEs, cm^{-1}) and vibrational frequencies (cm^{-1}) of La(C_2H_2) and La(C_5H_8) (Iso A) from MATI spectroscopy and DFT/B3LYP calculations. ν_n^+ and ν_n are vibrational modes in the ionic and neutral states.

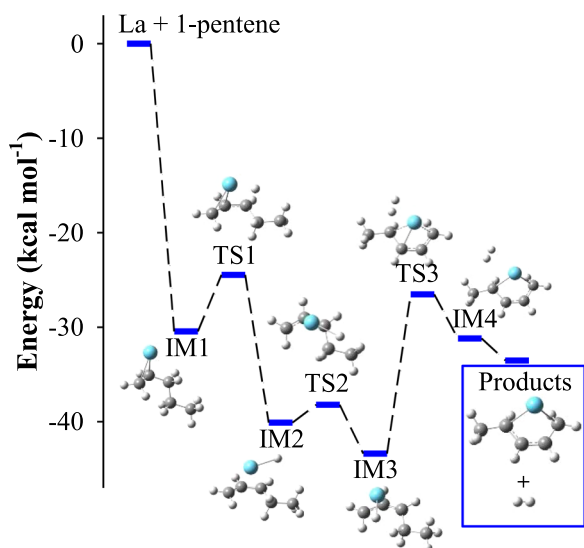| Complex	MATI	B3LYP	Mode description
La(C_2H_2), C_{2v}, $^1A_1 \leftarrow {}^2A_1$			
AIE	41 174	42 107	
ν_4^+	522	528	Symmetric La-ligand stretch
La(C_5H_8) (iso A), C_1, $^1A \leftarrow {}^2A$			
AIE	38 984	39 675	
ν_{36}^+/ν_{36}	130/128	125/134	CH_3 bend
ν_{35}^+/ν_{35}	156/165	158/158	CH_3 torsion
ν_{32}^+/ν_{32}	290/268	288/278	Asymmetric La-ligand stretch
ν_{30}^+/ν_{30}	410/402	405/385	Symmetric La-ligand stretch

FIG. 4. Reaction pathway and energy profile for the formation of La(C$_5$H$_8$) (Iso A) from the La + 1-pentene reaction calculated at the DFT/B3LYP level, where IMn stands for intermediates and TSn transition states.

The formation of Iso A is thermodynamically and kinetically favorable. Figures 4 and 5 present the DFT/B3LYP computed stationary points for the formation of the two isomers from the H$_2$ elimination of 1-pentene and 2-pentene, respectively. These stationary points include reactants, intermediates (IMn), transition states (TSn), and products in their doublet spin states. Tables S2 and S3 of the supplementary material report electronic energies without and with vibrational zero point energy corrections, enthalpies, and free energies of stationary points relative to those of reactants La + 1-/2-pentene. As expected, the relative enthalpy of each stationary point is close to the internal energy, which is the sum of the electronic energy with the zero point correction plus a small thermal energy at 298 K. The relative free energy is somewhat less negative than the enthalpy because the entropy is reduced
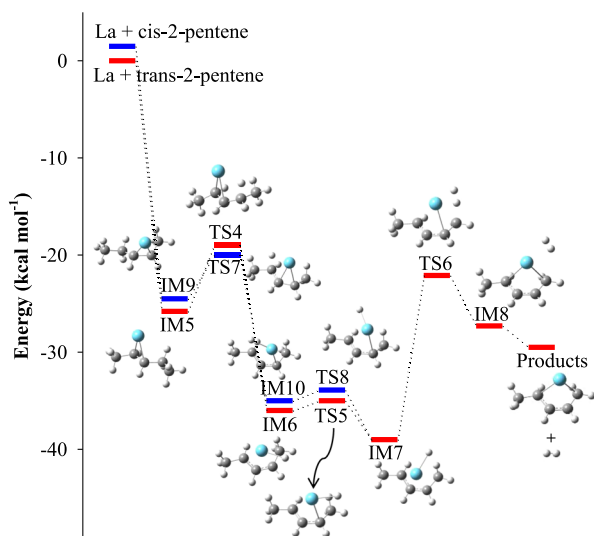

FIG. 5. Reaction pathways and energy profiles for the formation of La(C$_5$H$_8$) (Iso A) from the La + *cis*-2-pentene (blue) and *trans*-2-pentene (red) reactions calculated at the DFT/B3LYP level, where IMn stands for intermediates and TSn transition states.

from La + pentene to a local minimum or a transition state. We consider the concerted H$_2$ elimination because previous studies have shown that step-wise dehydrogenation paths are less favorable for the metal atom-mediated dehydrogenation of small alkenes and alkynes.[63,65–70,91–97]

A plausible reaction mechanism for the formation of Iso A from the La + 1-pentene reaction consists of La addition to the C=C double bond, La insertion into two C(sp^3—H) bonds, and concerted H$_2$ elimination (Fig. 4). The reaction begins with La atom addition to the C=C bond to form a π complex [La(CH$_2$CHCH$_2$CH$_2$CH$_3$), IM1] at 30.5 kcal mol^{-1} blow the reactants. Upon the La addition, the C=C bond of 1-pentene is elongated by 0.177 Å (from 1.332 Å to 1.509 Å) due to the cleavage of the π bond between the carbon atoms. The change from the C=C to C—C bond is also evidenced by the bending of the H atoms in the ethenyl group of the ligand. A molecular orbital analysis reveals that the unpaired pπ electron on each of the two ethenyl carbon atoms is paired with a La 5d electron to form a La—σ bond. Thus, the resultant π complex can be considered as a three-membered metallacycle. The exothermic energy from the La addition to 1-pentene (30.5 kcal mol^{-1}) is similar to those from La additions to ethylene (32.4 kcal mol^{-1}),[65] propene (29.7 kcal mol^{-1}),[67] and 1-butene (32.5 kcal mol^{-1})[70] but significantly lower than those from La additions to propyne (52.3 kcal mol^{-1})[63] and 1- and 2-butynes (52.4 and 51.1 kcal mol^{-1}).[69] Alkenes are generally not as good electrophiles as alkynes due to their higher-energy empty C 2pπ orbitals and tend to have weaker back electron donations from metal d orbitals than alkynes, which lead to slightly longer La—C bonds in lanthanacyclopropanes than those in lanthanacyclopropenes.[69] The weaker bonding between La and alkenes results in their lower exothermicity. The second step is the activation of two C(sp^3)-bonds by La insertion. The first insertion occurs at a C(sp^3)—H bond of the CH$_2$ group in the β position to form inserted species H—La—(η^3—CH$_2$CHCHC$_2$H$_5$) (IM2). IM2 is more stable than IM1 (by 9.6 kcal mol^{-1}) because La is in an η^3 binding mode rather than a η^2 mode. The La—H bond (2.089 Å) in IM2 rotates to form a slightly more stable IM3 (by 3.3 kcal mol^{-1}) where La-allylic carbon distances are slightly shorter (2.696 Å in IM2 and 2.667 A in IM3). The La—H rotation moves the H atom away so that it does not hinder the path for a second La insertion. The second insertion occurs at a C(sp^3)—H bond of the CH$_2$ group in the γ position to form IM4, which is 12.2 kcal mol^{-1} less stable than IM3. This is in contrast to the first insertion where the inserted species IM2 is more stable than the precursor IM1. In the first La insertion, the formation of the new La—H and La—C bonds in IM2 overcompensates the cleavage of a C—H bond in IM1, making the inserted species more stable. In the second La insertion, a new La—H bond is formed along with the shift of a La—C bond from β—C to γ—C in IM4. The resultant La—H bond is weaker than the cleaved C—H bond in IM3, resulting in the less stable IM4. IM4 may be considered as a dihydrogen complex because the L-bonded H—H distance (0.770 Å) is basically the same as the equilibrium H—H bond length (0.774 Å) in a free H$_2$ molecule. The final step is the concerted H$_2$ elimination from IM4 to form Iso A. The whole process La + 1-pentene → Iso

A is exothermic by 33.5 kcal mol^{-1} and has no overall energy barriers. Along the reaction coordinates, the activation of the C(sp^3)—H bonds in the (β, γ) positions is preferred over those in the (α, β) or (α,α′) positions because the later would lead to less stable 4- or 3-membered metallacycles (e.g., Iso C or Iso D). Because the transition states (TS1-TS3) are all considerably below the isolated reactants (La + 1-pentene) in energy, all intermediates (IM1-IM4) have a tendency to convert to the product (Iso A). This may explain why no intermediates were observed in our experiments even though the adduct (IM1) and inserted species (IM2, IM3) are more stable than the product. This observation is similar to the previous studies of La reactions with other small unsaturated hydrocarbons,[63,65,69,70] except for propene where a La-inserted species was identified.[67]

2-pentene dehydrogenation follows a similar path as 1-pentene. Because 2-pentene used in our experiment is a mixture of trans and cis conformers, we have considered the dehydrogenation of both conformers (Fig. 5: red for *trans*-2-pentene and blue for *cis*-2-pentene). In each case, the dehydrogenation path consists of La addition to the C=C double bond (IM5 or IM9), La insertion into a β C(sp^3—H) bond in the ethyl group (IM6 or IM10), La—H bond rotation (IM7), La

insertion into a β′ C(sp^3—H) bond in the methyl group (IM8), and finally H$_2$ elimination. The main difference between IM5 and IM9 is in the relative orientations of the ethyl groups, whereas that between IM6 and IM10 is in the orientations of the La—H bonds. Like the 1-pentene dehydrogenation, the whole process of the *cis*- or *trans*-2 pentene dehydrogenation is exothermic (by 29.5 or 28.0 kcal mol^{-1}) and has no energy barriers. On the other hand, the (β, β′) dehydrogenation is preferred over the (β, γ) dehydrogenation for *cis*- and *trans*-2-pentene because the (β, β′) carbon (sp^3) are in the proximity of the La atom and the γ carbon (sp^3) is further away. For the La(1-pentene) π complex, there is only one β position. After the cleavage of the first C(sp^3)—H bond in this position, the β carbon atom is changed from sp^3 to sp^2 hybridization. Similarly, the carbon atoms in the (α, α′) position are also in sp^2 hybridization. Activation of a C(sp^2)—H bond is generally less favorable than that of a C(sp^3)—H bond. Thus, a γ C (sp^3)—H bond is favored for the second La insertion of 1-pentene.

2-pentene may also undergo isomerization to 1-pentene prior to dehydrogenation. Possible isomerization pathways of *trans*- and *cis*-2-pentene are illustrated in Fig. 6 (red for *trans*-pentene and blue for *cis*-2-pentene), and energies of
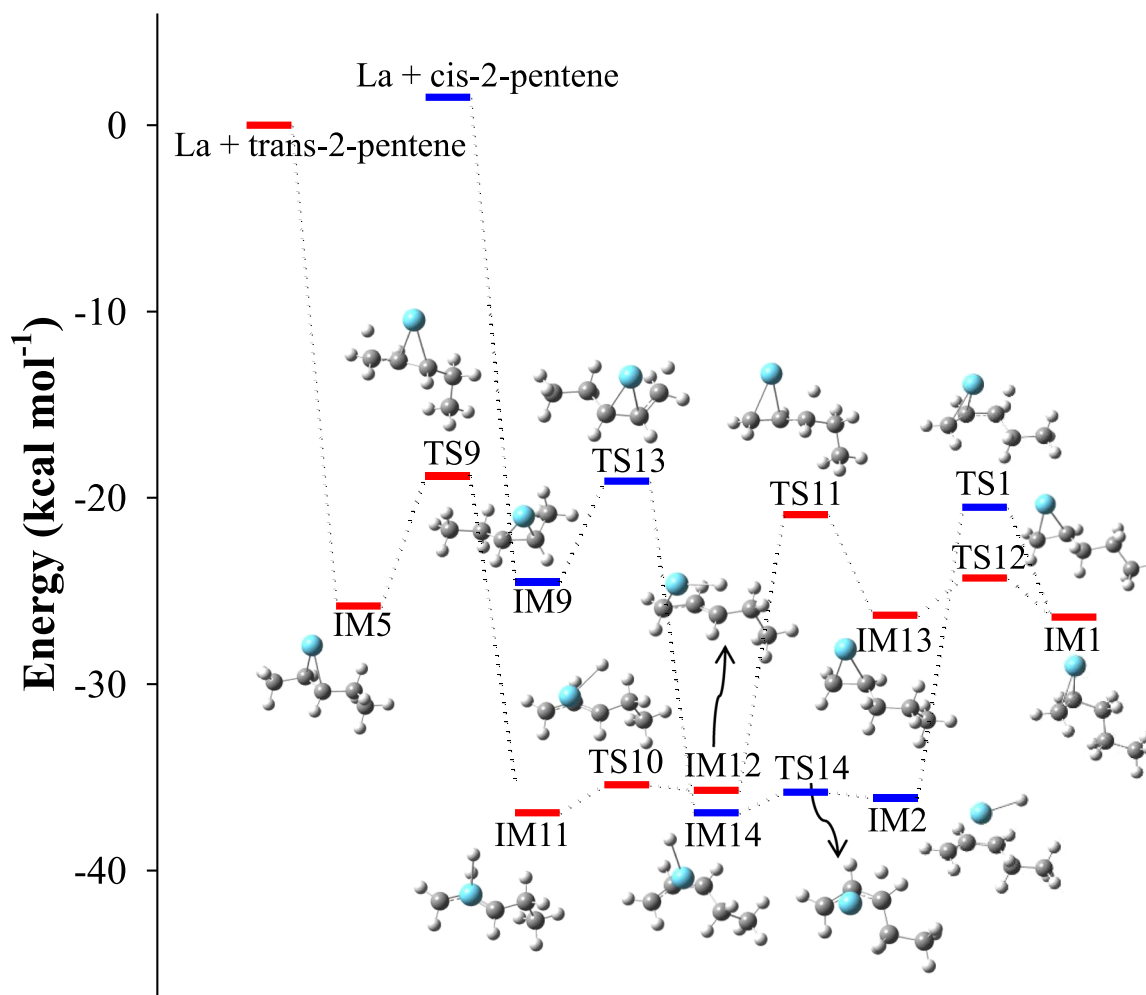
FIG. 6. Reaction pathways and energy profiles for the isomerization of La(CH$_3$CHCHCH$_2$CH$_3$) (IM5 or IM9) to La(CH$_2$CHCH$_2$CH$_2$CH$_3$) from the La + *cis*-2-pentene (blue) and *trans*-2-pentene (red) reactions calculated at the DFT/B3LYP level, where IMn stands for intermediates and TSn transition states.

the stationary points are summarized in Table S3 of the supplementary material. The *trans*-2-pentene to 1-pentene isomerization begins with La addition to the double bond to form La(2-pentene) π complex IM5, followed by La insertion into a C(cp³)—H bond of the methyl group that is adjacent to the double bond of 2-pentene to form inserted species IM11. In this species, La is in an η³-bonding mode with the allyl fragment. With La—H bond rotation via TS10, IM11 converts into another inserted species, IM12. IM12 then undertakes H migration from La to the carbon atom of the methine group to form La(1-pentene) π complex IM13, which converts into IM1 by rotating the C—C bond of the —CLaH—CH₂— group. The whole process is exothermic without any energy barrier. The isomerization of *cis*-2-pentene to 1-pentene is largely similar to the *trans*-2-pentene isomerization. The only difference is that the *cis*-2-pentene isomerization does not involve the C—C bond rotation, and IM1 is formed directly from the inserted species IM2 via the La-bonded H migration.

C. MATI spectroscopy, structure, and formation of La(C₂H₂)

Even though the number density of La(C₂H₂) is very low from both 1- and 2-pentene reactions (Fig. 1), we were able to obtain sharp MATI spectra for the species [Figs. 7(a) and 7(b)]. The spectra are a bit noisy but clearly show an origin band at 41 174 (5) cm⁻¹ and a weak vibronic band at ~522 cm⁻¹ above the origin band. The origin band position and the vibronic transitions are the same as those observed for La(C₂H₂) produced in the La reactions with ethylene and 1,3-butadiene.[65,66] The spectra can easily be assigned to the $^1A_1 \leftarrow {}^2A_1$ transition of lanthanacyclopropene by comparing with the spectra of La(C₂H₂) from the ethylene and 1,3-butadiene reactions[65,66] and the simulation in Fig. 7(c). The origin band corresponds to the AIE of the complex, and the 522 cm⁻¹ transition is due to the symmetric La—C₂H₂ stretch. The second quantum of the La—C₂H₂ stretch and the weak in-plane C—H bending transition around 832 cm⁻¹ in the simulation are not clearly present in the experimental spectra due to the low signal. The
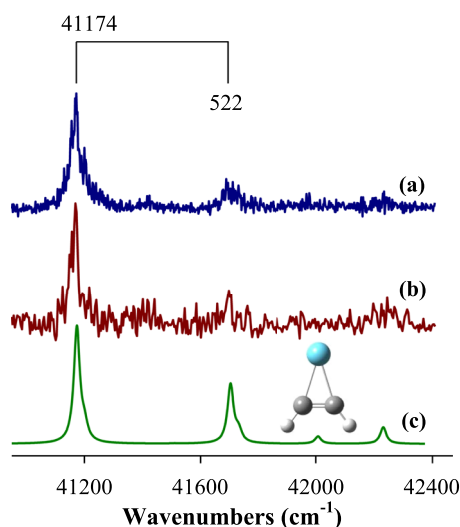
short FC profile observed in the MATI spectrum is due to very similar structures in the doublet and singlet states (Table S1 of the supplementary material).

A possible reaction path for the formation of La(C₂H₂) from the La + 1-pentene reaction is illustrated in Fig. 8. Like the dehydrogenation of 1-pentene (Fig. 4), the first step is La addition to the C═C bond to form a three-membered metallacyclopropane (IM1), which is the same species as the adduct formed in the dehydrogenation of the ligand. The second step is La insertion into the terminal α C(sp³)—H bond to form an inserted species (IM15) with the metal atom binding only to the α carbon atom. IM15 is different from the insertion species IM2 formed in the dehydrogenation of 1-pentene (Fig. 4), where La is in an η³-binding mode with the allylic group. The next step is the C(sp³)—C(sp³) bond cleavage leading to a tri-ligand La complex La(CHCH)(H)(CH₂CH₂CH₃) (IM16). Upon H migration from La to the propyl group, IM16 becomes a di-ligand La complex La(CHCH)(CH₃CH₂CH₃) (IM17), where the La binding with propane is very weak, whereas the La binding with the vinylene group is strong. Due to the weak propane binding, IM17 is easily decomposed to the La(C₂H₂) and C₃H₈ products. Along the reaction coordinates, the inserted species IM15 is slightly less stable than the three-membered metallacycle IM1 (by 3.4 kcal mol⁻¹) due to the replacement of a stronger La—C bond in IM1 by a weaker La—H bond in IM15.[12] Further down the reaction path, IM16 is even less stable than IM15 (by 9.2 kcal mol⁻¹) due to the cleavage of a C—C bond and the weakening of the La—H bond (from 2.087 Å in IM15 to 2.148 Å in IM16). This stability trend of the intermediates is reversed from IM16 to IM17, where the latter is more stable (by 7.9 kcal mol⁻¹). The lower energy of IM17 is largely due to the substitution of a weaker La—H bond in IM16 by a stronger C—H bond. The total energy of La(C₂H₂) + C₃H₈ is almost the same as that of IM17, which is expected as the La bonding with propane in IM17 is very weak. The whole process from the reactants to the products is exothermic by 33.5 kcal mol⁻¹. Kinetically, the reaction encounters two small energy barriers (TS16 and TS17 at 6.4

FIG. 7. MATI spectra of La(C₂H₂) produced from La reactions with 1-pentene [(a), blue] and 2-pentene [(b), dark red] and the simulation of the $^1A_1 \leftarrow {}^2A_1$ transition of La(C₂H₂) (C₂ᵥ) at 300 K [(c), green].
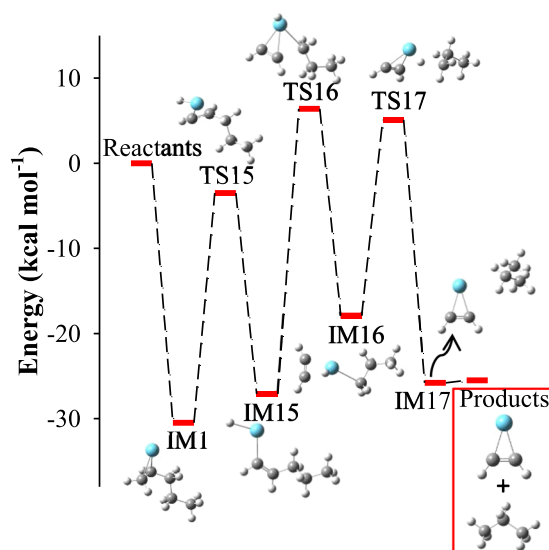

FIG. 8. Reaction pathway and energy profile for the formation of La(C₂H₂) (C₂ᵥ) from the La + 1-pentene reaction calculated at the DFT/B3LYP level, where IMn stands for intermediates and TSn transition states.

and 5.1 kcal mol^{-1}, respectively) associated with cleavages of the C—C and La—C bonds. But, these barriers may be overcome by the collision energy of the species seeded in the carrier gas.

The formation of La(C$_2$H$_2$) from the La + 2-pentene reaction may not follow a similar reaction path to that of the 1-pentene reaction. As discussed above, the reaction path for the 1-pentene reaction includes La addition to the C=C double bond, La insertion to the α C(sp^3)—H bond, C—C bond cleavage, and H migration. Unlike the C(sp^3)—C(sp^3) bond cleavage and H migration from La to carbon in the 1-pentene reaction, the C—C bond breakage in the 2-pentene reaction would occur at a much stronger C(sp^2)=C(sp^2) bond and the H migration would require the activation of the two C—H bonds of the methyl group at the β position in addition to the La—H bond. The requirement for breaking the stronger C=C and multiple C—H bonds makes the formation of La(C$_2$H$_2$) by the La + 2-pentene reaction very unfavorable. Thus, we envision that La(C$_2$H$_2$) observed in Fig. 1(b) is likely formed via 2-pentene to 1-pentene isomerization, followed by the same pathway as for the 1-pentene reaction.

We have also considered the formation of La(C$_2$H$_2$) by the La(C$_5$H$_8$) $\rightarrow$ La(C$_2$H$_2$) + C$_3$H$_6$ secondary reaction but found that this reaction is not favorable due to the high reaction endothermicity (32.4 kcal mol^{-1}) and energy barriers (30.4, 36.9, and 29.7 kcal mol^{-1} for TS18, TS19, and TS20, respectively), as shown in Fig. S2 and Table S2 of the supplementary material. The reaction is endothermic because it involves energy-costing C—C bond cleavage but no new bond formation. The high barriers arise from the activation of the C—H and La—C bonds (TS18), the C—C bond (TS19), or the La—C and La—H bonds (TS20).

IV. CONCLUSIONS

We have reported the MATI spectra and formation of La(C$_5$H$_8$) and La(C$_2$H$_2$) formed by the La-mediated dehydrogenation and C—C bond cleavage of 1-pentene and 2-pentene. The spectra of La(C$_5$H$_8$) from the two reactions are the same and exhibit a strong origin band and metal-ligand stretching and methyl group bending or torsional transitions. The spectra of La(C$_2$H$_2$) from the two reactions are also identical and display a strong origin band and a weak metal-ligand stretching band. La(C$_5$H$_8$) and La(C$_2$H$_2$) are identified as methyl-lanthanacyclopentene (C$_1$) and lanthanacyclopropane (C$_{2v}$), respectively. The ground state of each species is a doublet state with a La-based 6s^1 electron configuration, and the lowest-energy state of the corresponding ion is a singlet state upon the removal of the La 6s^1 electron. Because of the non-bonding nature of the La 6s^1 electron, ionization has a small effect on the geometry of the neutral state. The formation of La(C$_5$H$_8$) from the two reactions consists La addition to the C=C double bond, La insertion into two C(sp^3)—H bonds, and concerted H$_2$ elimination. For the 2-pentene reaction, the formation of La(C$_5$H$_8$) may also involve 2-pentene to 1-pentene isomerization. In addition to the La addition and insertion, the formation of La(C$_2$H$_2$) from the 1-pentene reaction includes the C(sp^3)—C(sp^3) cleavage and H migration from La to C(sp^3), whereas the metallacyclopropene from

the 2-pentene reactions requires the ligand isomerization to 1-petnene.

SUPPLEMENTARY MATERIAL

See supplementary material for the geometries of the La(C$_5$H$_8$) and La(C$_2$H$_2$), the electronic energies, enthalpies, and free energies of the stationary points along the reaction coordinates for the formation of the two species, simulations of four higher-energy La(C$_5$H$_8$) isomers, and the reaction pathway and energy profile for the formation of La(C$_2$H$_2$) by the La(C$_5$H$_8$) decomposition.

[1] J. A. Labinger and J. E. Bercaw, Nature **417**, 507 (2002).
[2] R. G. Bergman, Nature **446**, 391 (2007).
[3] R. H. Crabtree, Chem. Rev. **110**, 575 (2010).
[4] T. B. Marder, P. W. Dyer, I. J. S. Fairlamb, S. Gibson, and P. Scott, Dalton Trans. **39**, 10321 (2010).
[5] J. Wencel-Delord, T. Droge, F. Liu, and F. Glorius, Chem. Soc. Rev. **40**, 4740 (2011).
[6] M. P. Doyle and K. I. Goldberg, Acc. Chem. Res. **45**(6), 777 (2012).
[7] P. L. Arnold, M. W. McMullon, J. Rieb, and F. E. Kuhn, Angew. Chem., Int. Ed. **54**, 82 (2015).
[8] R. H. Crabtree and A. Lei, Chem. Rev. **117**, 8481 (2017), Thematic Issue on CH Activation.
[9] J. F. Hartwig, Acc. Chem. Res. **50**, 549 (2017), Special Issue on Holy Grails in Chemistry, Part II.
[10] K. Eller and H. Schwarz, Chem. Rev. **91**, 1121 (1991).
[11] D. Schroeder and H. Schwarz, Angew. Chem., Int. Ed. **34**, 1973 (1995).
[12] *Organometallic Ion Chemistry*, edited by B. S. Freiser (Kluwer, Dordrecht, 1996).
[13] D. K. Bohme and H. Schwarz, Angew. Chem., Int. Ed. **44**, 2336 (2005).
[14] J. Roithova and D. Schroeder, Chem. Rev. **110**, 1170 (2010).
[15] H. Schwarz, Angew, Chem., Int. Ed. **50**, 10096 (2011).
[16] H. Schwarz, Isr. J. Chem. **54**, 1413 (2014).
[17] P. B. Armentrout, Catal. Sci. Technol. **4**, 2741 (2015).
[18] H. Schwarz, Angew. Chem., Int. Ed. **54**, 10090 (2015).
[19] P. B. Armentrout, Int. J. Mass Spectrom. **377**, 54 (2015).
[20] M. T. Rodgers and P. B. Armentrout, Chem. Rev. **116**, 5642 (2016).
[21] P. B. Armentrout, Chem. - Eur. J. **23**, 10 (2017).
[22] J. J. Schroden and H. F. Davis, "Modern trend in chemical dynamics. Part II: Experiment and theory," in *Advanced Series in Physical Chemistry*, edited by X. Yang and K. Lium (World Scientific, Singapore, 2004), Vol. 14, p. 215.
[23] J. C. Weisshaar, Acc. Chem. Res. **26**, 213 (1993).
[24] B. T. Qiao, A. Q. Wang, X. F. Yang, L. F. Allard, Z. Jiang, Y. T. Cui, J. Y. Liu, J. Li, and T. Zhang, Nat. Chem. **3**, 634 (2011).
[25] G. Kyriakou, M. B. Boucher, A. D. Jewell, E. A. Lewis, T. J. Lawton, A. E. Baber, H. L. Tierney, M. Flytzani-Stephanopoulos, and E. C. Sykes, Science **335**, 1209 (2012).
[26] A. Figueroba, G. Kovacs, A. Bruix, and K. M. Neyman, Catal. Sci. Technol. **6**, 6806 (2016).
[27] J. Jones, H. Xiong, A. T. DeLaRiva, E. J. Peterson, H. Pham, S. R. Challa, G. Qi, S. Oh, M. H. Wiebenga, X. I. Pereira Hernandez, Y. Wang, and A. K. Datye, Science **353**, 150 (2016).
[28] W. Liu, L. X. Zhang, W. Yan, X. Liu, X. Yang, S. Miao, W. Wang, A. Wang, and T. Zhang, Chem. Sci. **7**, 5758 (2016).
[29] J. Y. Liu, ACS Catal. **7**, 34 (2017).
[30] G. X. Pei, X. Y. Liu, X. F. Yang, L. L. Zhang, A. Q. Wang, L. Li, H. Wang, X. D. Wang, and T. Zhang, ACS Catal. **7**, 1491 (2017).

[31] S. Yang, J. Kim, Y. J. Tak, A. Soon, and H. Lee, Angew. Chem., Int. Ed. **55**, 2058 (2016).

[32] B. Zhang, H. Asakura, J. Zhang, J. G. Zhang, S. De, and N. Yan, Angew. Chem., Int. Ed. **55**, 8319 (2016).

[33] R. Lang, T. B. Li, D. Matsumura, S. Miao, Y. J. Ren, Y. T. Cui, Y. Tan, B. T. Qiao, L. Li, A. Q. Wang, X. D. Wang, and T. Zhang, Angew. Chem., Int. Ed. **55**, 16054 (2016).

[34] L. B. Wang, W. B. Zhang, S. P. Wang, Z. H. Gao, Z. H. Luo, X. Wang, R. Zeng, A. W. Li, H. L. Li, M. L. Wang, X. S. Zheng, J. F. Zhu, W. H. Zhang, C. Ma, R. Si, and J. Zeng, Nat. Commun. **7**, 14036 (2016).

[35] X. F. Yang, A. Q. Wang, B. T. Qiao, J. Li, J. Y. Liu, and T. Zhang, Acc. Chem. Res. **46**, 1740 (2013).

[36] A. Wang, J. Li, and T. Zhang, Nat. Rev. Chem. **2**, 65 (2018).

[37] R. S. Walters, T. D. Jaeger, and M. A. Duncan, J. Phys. Chem. A **106**, 10482 (2002).

[38] R. S. Walters, E. D. Pillai, P. v. R. Schleyer, and M. A. Duncan, J. Am. Chem. Soc. **127**, 17030 (2005).

[39] R. S. Walters, P. V. Schleyer, C. Corminboeuf, and M. A. Duncan, J. Am. Chem. Soc. **127**, 1100 (2005).

[40] A. D. Brathwaite, T. B. Ward, R. S. Walters, and M. A. Duncan, J. Phys. Chem. A **119**, 5658 (2015).

[41] R. B. Metz, Int. Rev. Phys. Chem. **23**, 79 (2004).

[42] R. B. Metz, Adv. Chem. Phys. **138**, 331 (2008).

[43] G. Altinay, M. Citir, and R. B. Metz, J. Phys. Chem. A **114**, 5104 (2010).

[44] G. Altinay and R. B. Metz, J. Am. Soc. Mass Spectrom. **21**, 750 (2010).

[45] G. Altinay and R. B. Metz, Int. J. Mass spectrom. **297**, 41 (2010).

[46] M. Citir, G. Altinay, G. Austein-Miller, and R. B. Metz, J. Phys. Chem. A **114**, 11322 (2010).

[47] G. Altinay, A. Kocak, J. S. Daluz, and R. B. Metz, J. Chem. Phys. **135**, 084311 (2011).

[48] M. Perera, P. Ganssle, and R. B. Metz, Phys. Chem. Chem. Phys. **13**, 18347 (2011).

[49] A. Kocak, M. A. Ashraf, and R. B. Metz, J. Phys. Chem. A **119**, 9653 (2015).

[50] A. Kocak, Z. Sallese, M. D. Johnston, and R. B. Metz, J. Phys. Chem. A **118**, 3253 (2014).

[51] M. A. Ashraf, C. W. Copeland, A. Kocak, A. R. McEnroe, and R. B. Metz, Phys. Chem. Chem. Phys. **17**, 25700 (2015).

[52] T. B. Ward, A. D. Brathwaite, and M. A. Duncan, Top. Catal. **61**, 49 (2018).

[53] V. J. F. Lapoutre, B. Redlich, A. F. G. van der Meer, J. Oomens, J. M. Bakker, A. Sweeney, A. Mookherjee, and P. B. Armentrout, J. Phys. Chem. A **117**, 4115 (2013).

[54] O. W. Wheeler, M. Salem, A. Gao, J. M. Bakker, and P. B. Armentrout, J. Phys. Chem. A **120**, 6216 (2016).

[55] S. R. Miller, T. P. Marcy, E. L. Millam, and D. G. Leopold, J. Am. Chem. Soc. **129**, 3482 (2007).

[56] W. Y. Lu, P. D. Kleiber, M. A. Young, and K. H. Yang, J. Chem. Phys. **115**, 5823 (2001).

[57] A. S. Gentlman, A. E. Green, D. R. Price, E. M. Cunningham, A. Iskra, and S. R. Mackenzie, Top. Catal. **61**, 81 (2018).

[58] D. J. Brugh, R. S. Dabell, and M. D. Morse, J. Chem. Phys. **121**, 12379 (2004).

[59] M. A. Garcia and M. D. Morse, J. Phys. Chem. A **117**, 9860 (2013).

[60] D. J. Brugh and M. D. Morse, J. Chem. Phys. **141**, 064304 (2014).

[61] E. L. Johnson and M. D. Morse, Mol. Phys. **113**, 2255 (2015).

[62] M. A. Flory, A. J. Apponi, L. N. Zack, and L. M. Ziurys, J. Am. Chem. Soc. **132**, 17186 (2010).

[63] D. Hewage, M. Roudjane, W. R. Silva, S. Kumari, and D.-S. Yang, J. Phys. Chem. A **119**, 2857 (2015).

[64] D. Hewage, W. R. Silva, W. Cao, and D.-S. Yang, J. Am. Chem. Soc. **138**, 2468 (2016).

[65] S. Kumari, W. Cao, Y. Zhang, M. Roudjane, and D.-S. Yang, J. Phys. Chem. A **120**, 4482 (2016).

[66] D. Hewage, W. Cao, J. H. Kim, Y. Wang, Y. Liu, and D.-S. Yang, J. Phys. Chem. A **121**, 1233 (2017).

[67] S. Kumari, W. Cao, D. Hewage, R. Silva, and D.-S. Yang, J. Chem. Phys. **146**, 074305 (2017).

[68] D. Hewage, W. Cao, S. Kumari, R. Silva, T. H. Li, and D.-S. Yang, J. Chem. Phys. **146**, 184304 (2017).

[69] W. Cao, D. Hewage, and D.-S. Yang, J. Chem. Phys. **147**, 064303 (2017).

[70] W. Cao, D. Hewage, and D.-S. Yang, J. Chem. Phys. **148**, 044312 (2018).

[71] Y. Zhang, M. W. Schmidt, S. Kumari, M. S. Gordon, and D.-S. Yang, J. Phys. Chem. A **120**, 6963 (2016).

[72] P. B. Armentrout, L. F. Halle, and J. L. Beauchamp, J. Am. Chem. Soc. **103**, 6624 (1981).

[73] M. A. Hanratty, C. M. Paulsen, and J. L. Beauchamp, J. Am. Chem. Soc. **107**, 5074 (1985).

[74] J. B. Schilling and J. L. Beauchamp, Organometallics **7**, 194 (1988).

[75] L. M. Lech and B. S. Freiser, Organometallics **7**, 1948 (1988).

[76] R. L. Hettich and B. S. Freiser, Organometallics **8**, 2447 (1989).

[77] D. A. Peake, M. L. Gross, and D. P. Ridge, J. Am. Chem. Soc. **106**, 4307 (1984).

[78] D. A. Peake and M. L. Gross, J. Am. Chem. Soc. **109**, 600 (1987).

[79] P. Mourgues, A. Ferhati, T. B. McMahon, and G. Ohanessian, Organometallics **16**, 210 (1997).

[80] B. R. Sohnlein, S. G. Li, J. F. Fuller, and D.-S. Yang, J. Chem. Phys. **123**, 014318 (2005).

[81] C. E. Moore, *Atomic Energy Levels* (National Bureau of Standards, Washington, DC, 1971).

[82] M. A. Duncan, T. G. Dietz, and R. E. Smalley, J. Chem. Phys. **75**, 2118 (1981).

[83] A. D. Becke, J. Chem. Phys. **98**, 5648 (1993).

[84] R. Krishnan, J. S. Binkley, R. Seeger, and J. A. Pople, J. Chem. Phys. **72**, 650 (1980).

[85] M. Dolg, H. Stoll, A. Savin, and H. Preuss, Theor. Chim. Acta **75**, 173 (1989).

[86] D. S. Yang, J. Phys. Chem. Lett. **2**, 25 (2011).

[87] M. J. Frish, G. W. Trucks, H. B. Schlegel, G. E. Scuseria, M. A. Robb, J. R. Cheeseman, G. Scalmani, V. Barone, B. Mennucci, G. A. Petersson, H. Nakatsuji, M. Caricato, X. Li, H. P. Hratchian, A. F. Izmaylov, J. Bloino, and G. Zheng, GAUSSIAN 09, Revision A.01, Gaussian, Inc., Wallingford, CT, 2009.

[88] S. Li, "Threshold photoionization and ZEKE photoelectron spectroscopy of metal complexes," Ph.D. thesis, University of Kentucky, 2004.

[89] E. V. Doktorov, I. A. Malkin, and V. I. Man'ko, J. Mol. Spectrosc. **64**, 302 (1977).

[90] F. Duschinsky, Acta Physicochim. **7**, 551 (1937).

[91] Y. Wen, M. Porembski, T. A. Ferrett, and J. C. Weisshaar, J. Phys. Chem. A **102**, 8362 (1998).

[92] M. Porembski and J. C. Weisshaar, J. Phys. Chem. A **105**, 6655 (2001).

[93] R. Z. Hinrichs, J. J. Schroden, and H. F. Davis, J. Phys. Chem. A **107**, 9284 (2003).

[94] T. H. Li and X. G. Xie, J. Phys. Org. Chem. **23**, 768 (2010).

[95] R. Z. Hinrichs, J. J. Schroden, and H. F. Davis, J. Phys. Chem. A **112**, 3010 (2008).

[96] T. H. Li, C. M. Wang, S. W. Yu, X. Y. Liu, H. Fu, and X. G. Xie, J. Mol. Struct.: THEOCHEM **915**, 105 (2009).

[97] P.-P. Ma, Y.-C. Wang, W.-X. Wang, Z.-P. Deng, G.-P. Niu, X.-L. Wang, S. Li, and Y.-W. Zhang, Comput. Theor. Chem. **1085**, 23 (2016).